Journal of the European Ceramic Society 20 (2000) 215–225

Structural characterisation of silicon carbonitride ceramics derived from polymeric precursors

Stephan Traßl[a], Daniel Suttor[a], Günter Motz[a], Ernst Rössler[b,*], Günter Ziegler[a]

[a]*Institut für Materialforschung (IMA I), Universität Bayreuth, 95440 Bayreuth, Germany*
[b]*Physikalisches Institut (EP II), Universität Bayreuth, 95440 Bayreuth, Germany*

Received 31 December 1998; accepted 21 April 1999

Abstract

Polymeric precursors with tailored structures were prepared from functionalised chlorosilanes. Pyrolysis under inert atmospheres led to amorphous Si–C–N–(H) ceramics at 1000°C. Further heat treatment caused the transformation into the thermodynamically stable crystalline phase assemblage. The structural changes associated with crosslinking, pyrolysis and crystallisation were studied by characterising the solid intermediates between 300 and 1600°C applying ^{29}Si and ^{13}C solid state nuclear magnetic resonance (NMR) spectroscopy. In addition, Fourier transformed infrared (FTIR) spectroscopy, X-ray diffraction (XRD), thermoanalytical techniques and density measurements were employed. The combination of these methods and the use of polymeric precursors with tailored structures pointed to a correlation of the polymer architecture with the structure of the amorphous ceramic material.

Keywords: Precursors-organic; Spectroscopy; Silicon carbonitride; Characterisation; Si–C–N

1. Introduction

High performance ceramics such as SiC and Si_3N_4 are known as materials with high strength and hardness, low thermal expansion coefficient and good oxidation resistance. These ceramics are produced predominantly via powdermetallurgical processes, using sintering aids and/or high pressure in order to simplify consolidation of these covalent materials at temperatures up to 2000°C. Sintering additives, however, will eventually yield a glass phase at grain boundaries and triple points, hence degrading the high temperature properties.[1,2]

Based on the work of Verbeek and Winter[3] as well as Yajima[4] in the 1970s, considerable interest was focused on the pyrolysis of preceramic polymers. In comparison to conventional processes, the precursor method offers some important advantages: (i) low impurity level; (ii) homogeneous element distribution; (iii) low processing temperatures; and (iv) flexible forming methods.[5–10] Hence, in the last decades a whole variety of such precursors were synthesised and the pyrolysis products characterised.[11–18] Thermal or catalytic activated crosslinking of the preceramic oligomers first provides an unmeltable and insoluble 3-D network. These highly crosslinked polymers can be converted into ceramics via pyrolysis at temperatures up to 1000°C. At higher temperatures the amorphous structure crystallises to thermodynamically stable phases, in the case of carbon rich polysilazanes to SiC, Si_3N_4 and C.[12,19–21]

The conversion of the polymer into an amorphous ceramic material and the amorphous material into a crystalline ceramic is a very complex process and so far only little understood. Especially the correlation between the precursor architecture and the structure of the amorphous material and the effect of the structure on the crystallisation behaviour is not known. In order to utilise the full potential of the precursor route, however, a detailed understanding of the structural changes is important. Hence, polymers with different architectures must be used and, therefore, a detailed understanding of the synthesis of such polymers is necessary.

---

* Corresponding author. Tel.: +49-921-55-2606; fax: +49-921-55-2621.

PII: S0955-2219(99)00142-9

Most publications on polymer pyrolysis are dealing with the characterisation of only one precursor, often exhibiting varying structural units within the polymer or even consisting of polymer blends.[19,20,22–27] Crosslinking mechanisms, taking into account functional groups and crosslinking conditions (temperature, atmosphere, catalyst) were also examined.[18,28,29] Furthermore, the pyrolysis behaviour of different types of precursors such as silanes, carbosilanes, carbosilazanes and silsesquioxanes was compared with regard to e.g. the carbon content or the microstructural development of the ceramic material.[30,31] Only little data have been presented with respect to the comparison of different systems. One example was given by Seitz et al. characterising commercially available silazanes (NCP 200, Nichimen Corp., Japan and VT 50, Hoechst, Germany) via NMR spectroscopy.[32] The precursors consisted of different molecular units with NCP 200 containing silicon atoms bonded to two bridging nitrogens and VT 50 containing silicon atoms bonded to three bridging nitrogens. The amorphous materials showed significant structural differences between the VT 50 derived ceramic residue exhibiting a high amount of sp^2-carbon and SiN_4 sites and the NCP 200 pyrolysis residue yielding various SiC_xN_y-sites.

In order to get a more detailed understanding of the structural changes of the pyrolysis process, the use of various and complementary characterisation methods, especially spectroscopic, is important. FTIR spectroscopy is used for studying the decomposition mechanisms of the polymer, providing information on the presence of functional groups. The most powerful tool to investigate all stages during pyrolysis is solid state NMR spectroscopy. Because of probing the atomic coordination, the resolution of the NMR spectra is often high enough to allow the determination of the local chemical structure. Elastic neutron scattering is another method for investigating amorphous materials. However, it is very difficult to extract the structure from the scattering data, because they are not unique enough to favor a single structure, since no Bragg reflection applies. Due to measurement problems when using solid state ^{13}C-NMR of unhydrogenated carbon samples (no proton enhancement possible) in order to study the role of excess carbon (not bonded to silicon) in the sample, Raman spectroscopy can be used in addition to overcome this difficulties. This method is very sensitive with respect to the modification of disordered carbon. Especially X-ray diffraction (XRD) is applied to characterise the crystallisation behaviour of the amorphous materials when crystalline phases are present. Scanning electron microscopy (SEM) and transmission electron microscopy (TEM) allows characterisation of the microstructural development and also crystallisation behaviour. Additional information on the local chemistry can be derived by detecting unpaired electrons via ESR spectroscopy, from chemical analysis to get the elemental composition, from bulk density measurements and from analysing the gaseous species evolving during pyrolysis via coupled TG (thermogravimetry)/FTIR or TG/MS (mass spectroscopy) measurements.

In this paper, we report on the characterisation of the ceramisation process starting with three polymers with different structure in order to compare the microstructural evolution. For this purpose, we combine the results received, in particular, from ^{29}Si- and ^{13}C-solid state nuclear magnetic resonance (NMR) spectroscopy, Fourier transformed infrared (FTIR) spectroscopy, X-ray diffraction (XRD), thermoanalytical techniques and density measurements.

2. Experimental procedure

The starting silazanes were synthesised from di- and trifunctionalised chlorosilanes as reported elsewhere.[17] The preceramic oligomers are described in Table 1 and Fig. 1.

According to conventional silicon nomenclature, we classify the basic units of the silazanes based on the number of bridging nitrogens. Acronyms used are: T ($-Si(NH)_{1.5}$) and D ($=Si(NH)$). The liquid oligomer VN contains $[-CH_3CH=CH_2Si(NH)]$ units (according to our classification D-units), forming mainly six- and eight-membered cyclics. The silazane TVS consists of the T-units $[-CH=CH_2Si(NH)_{1.5}]$. Here, each silicon is bridged via three nitrogens with another silicon. Therefore the precursor is already crosslinked to yield a 3-D network resulting in a meltable and soluble solid. The precursor HVNG with the structure $[-CH=CH_2Si(NH)_{1.5}]_x[-HCH_3Si(NH)]_y$ ($x{:}y=1{:}1$) is a silazane with mixed T- and D-units. The oligomer HVN has the same structure as HVNG, but exhibits a reduced vinyl content. The precursors were crosslinked in general by using DCP (dicumylperoxide) as a catalyst and subsequent thermal treatment at 300°C for 5 h in N_2-atmosphere. For all experiments, powder samples were used. Powders were obtained from the as received unmeltable solids using a ball mill and zirconia milling media. The powders were sieved and the fraction $<125\ \mu m$ used for thermal treatments up to 1600°C ($\Delta T = 100\,K$).

Table 1
Structural units of the precursors TVS, VN, HVNG and HVN[a]

$[-R^1Si(NH)_{1.5}]$	(T-unit)	TVS
$[-R^1R^2Si(NH)]$	(D-unit)	VN
$[-R^1Si(NH)_{1.5}]_x[-R^3R^2Si(NH)]_y$		HVNG ($x{:}y=1{:}1$)
		HVN ($x{:}y=1{:}10$)
(T-unit)	(D-unit)	

[a] R^1: $CH=CH_2$; R^2: CH_3; R^3: H.

Bulk density measurements were performed using a helium pycnometer (AccuPyc 1330, Micromeritics). Structural changes which occur during annealing between room temperature (RT) and 1600°C were investigated in particular by NMR spectroscopy. ^{1}H-, ^{13}C- and ^{29}Si-liquid NMR spectra were recorded (ARX 250, Bruker) to characterise the preceramic polymers. The solvent used was C_6D_6. ^{13}C- and ^{29}Si-NMR spectra of the solid intermediates between 300 and 1600°C were obtained on a Bruker AVANCE DSX 400 spectrometer applying the magic angle spinning technique (MAS) with spinning rates of 5–7 kHz. From RT to 700°C a signal to noise enhancement using the cross polarisation (CP) method (^{1}H 90° pulse of 3.5 μs, contact time 5 ms, recycle delay 10 s) was possible due to the presence of a sufficient amount of protons in these samples. For powders heated above 700°C, the CP method became inefficient since the proton concentration was too low. Therefore single pulse excitation (90° pulse of 3 μs, recycle delay 10 min) was employed for recording ^{29}Si spectra in the latter case. ^{13}C spectra were recorded with a depth pulse excitation (90° pulse of 3 μs, recycle delay 60 s) in this case ($T > 700$°C), in order to avoid the ^{13}C signal from the sample holder.[33] The chemical shift data in the ^{1}H-, ^{13}C- and ^{29}Si-NMR spectra are listed with respect to TMS (tetramethylsilane) as an external standard. For further information, FTIR spectroscopy (transmission mode) was used employing a Bruker VECTOR 22 spectrometer and KBr pellets. The gaseous species evolving during pyrolysis were investigated with a coupled TG–FTIR set-up. Powder samples were annealed in a Netzsch STA 409 thermobalance and FTIR absorption spectra of the volatile species were recorded using a heated transmission line. X-ray diffraction (XRD) studies were executed on a Seifert XRD 3000 P powder diffractometer using Cu$_{K\alpha}$ radiation to detect crystalline phases in the pyrolytic residues above 1300°C.

3. Results and discussion

3.1. Structure of the precursor HVNG

The use of both di- and trifunctionalised chlorosilanes for synthesis yields a complex structure of the precursor. Therefore, no sharp lines in the ^{1}H-NMR spectrum are seen. The observed signals are assigned to $\equiv$Si–**CH**$_3$ (−0.15–0.4 ppm), Si–**NH**–Si (0.5–1.1 ppm), Si–**H** (4.4–5.0 ppm) and $\equiv$Si–**CH**$=$**CH**$_2$ (5.5–6.3 ppm) environments.[18,20,36] The ^{13}C-spectrum obtained from liquid NMR shows three peaks which are due to the presence of $\equiv$Si–**C**H$_3$ units (3.8 ppm) and the two carbons of the $\equiv$Si–**C**H$=$**C**H$_2$ group (132 ppm (Si–**C**H$=$), 140 ppm ($=$**C**H$_2$)).[18,19,23] Two signals appear in the ^{29}Si-spectrum. The position at −33.5 ppm is assigned to Si in the T-unit ((N)$_3$**Si**CH$=$CH$_2$). The signal between −18 and −24 ppm is caused by Si in the D-unit ((N)$_2$**Si**(H)CH$_3$)).[18] The ^{29}Si shifts indicate the formation of cyclic molecules with different ring size and/or different constituting elements

Table 2
FTIR absorption bands of the precursor HVNG

Wavenumber (cm^{-1})	Assignment
3390	ν (N–H)
3050, 3009	ν (C$_{Vi}$–H)
2963, 2900	ν (C$_{me}$–H)
2125	ν (Si–H)
1594, 1404	ν (C=C)
1255	δ (Si–CH$_3$)
1193, 1168	δ (N–H)

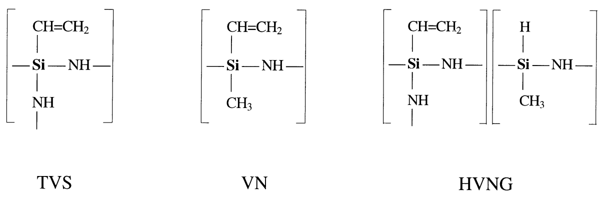

Fig. 1. Structural units of the precursors TVS, VN and HVNG.

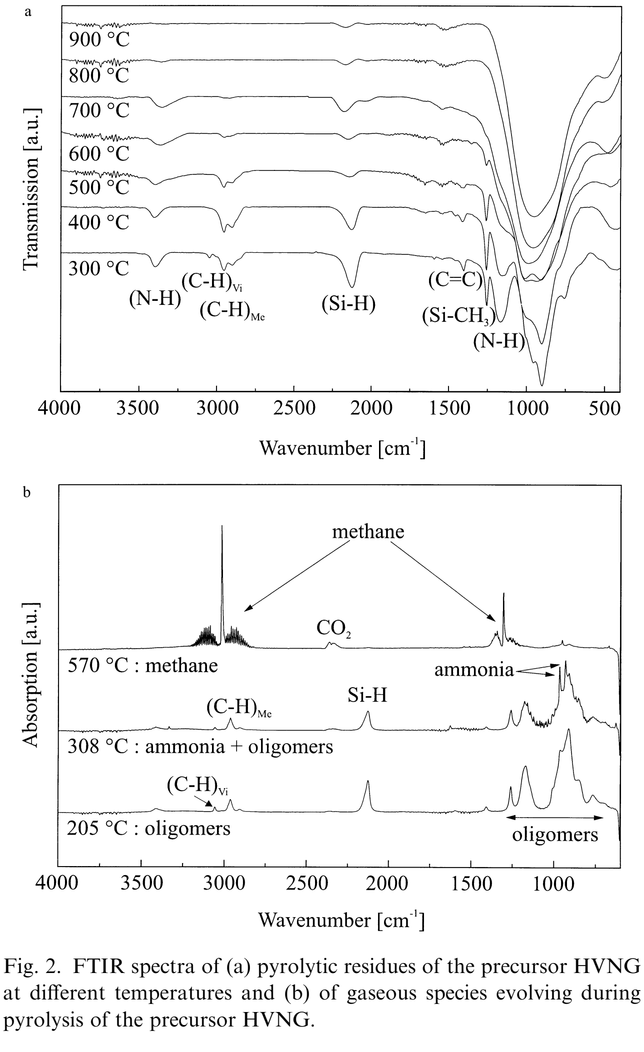

Fig. 2. FTIR spectra of (a) pyrolytic residues of the precursor HVNG at different temperatures and (b) of gaseous species evolving during pyrolysis of the precursor HVNG.

(3/4-T/D units) already crosslinked among each other. In fact, upon thermal treatment of this precursor without prior crosslinking, the evolution of low-molecular-weight oligomers was monitored via TG–FTIR measurements at temperatures below 300°C. FTIR spectroscopy was performed in order to identify the functional groups of the preceramic oligomer. The main absorption bands observed in the spectrum and their identification are given in Table 2.[17]

*3.2. Crosslinking mechanism and ceramisation of the precursor HVNG (*T = *300–700°C)*

The effect of crosslinking and the decomposition of the polymer network during pyrolysis were monitored by FTIR spectroscopy and coupled TG–FTIR measurements, Fig. 2(a) and (b). Thermal crosslinking at 300°C involves a mass loss of about 5% due to the evolution of volatile oligomers in addition to ammonia (crosslinking via transamination), Fig. 2(b). After this step the FTIR spectrum showed the absorption bands characteristic for the initial precursor. The intensity of the bands corresponding to N–H (3400, 1164 cm^{-1}), C–H (Me) (2953, 2898 cm^{-1}) and Si–CH_3 (1260 cm^{-1}) remained unchanged.[34] On the other hand, the intensity of those peaks assigned to Si–H (2125 cm^{-1}) and $-CH{=}CH_2$ (3047, 3009, 1406 cm^{-1}) decreased, indicating that crosslinking occurs via hydrosilylation and/or polymerisation, but is not yet completed.[34] Further heating up to 700°C resulted in a decrease of the intensity of all absorption bands due to the decomposition of the polymer. The dominant

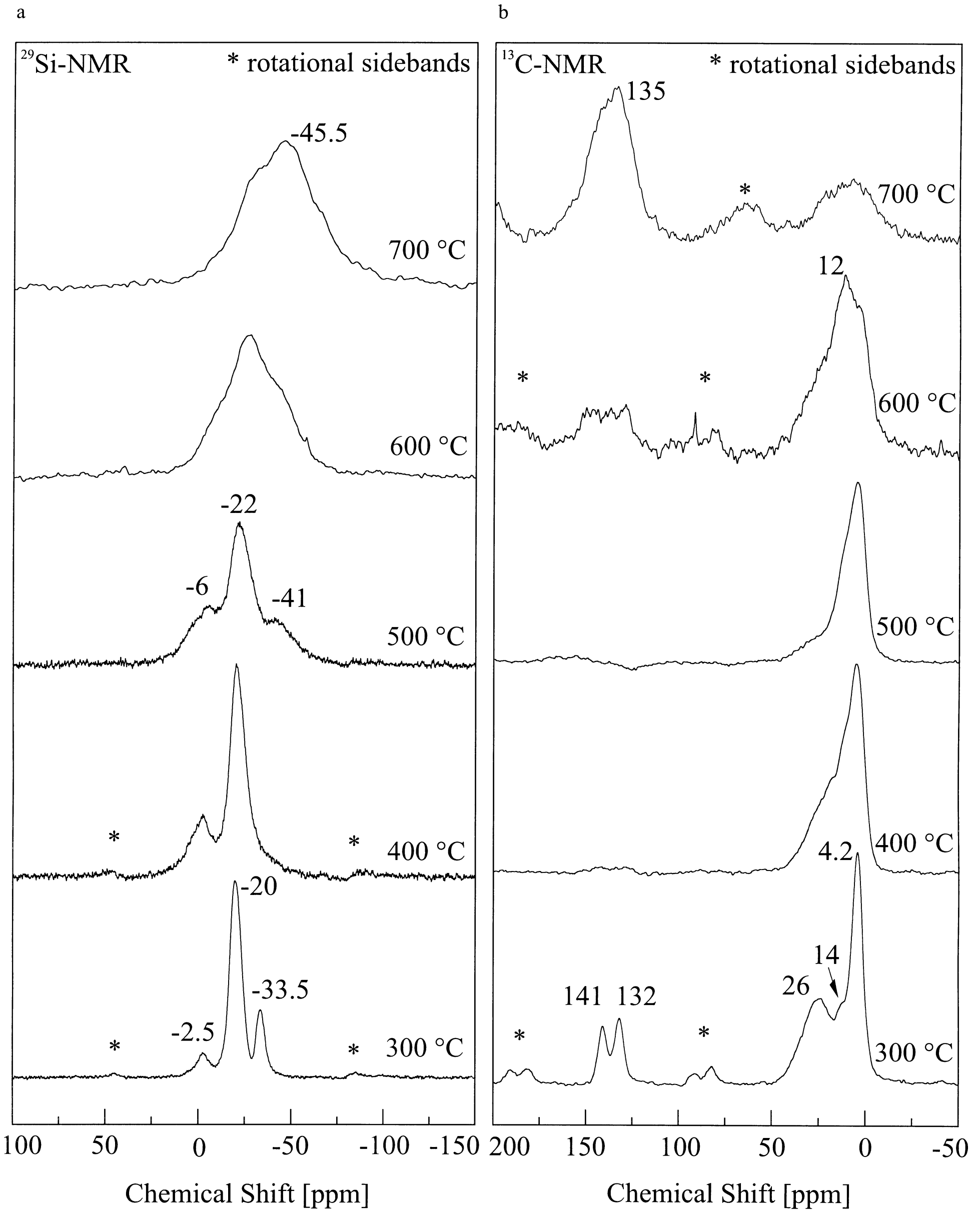

Fig. 3. (a) ^{29}Si- and (b) ^{13}C-NMR spectra of HVNG-derived powder samples heat treated at temperatures between 300 and 700°C.

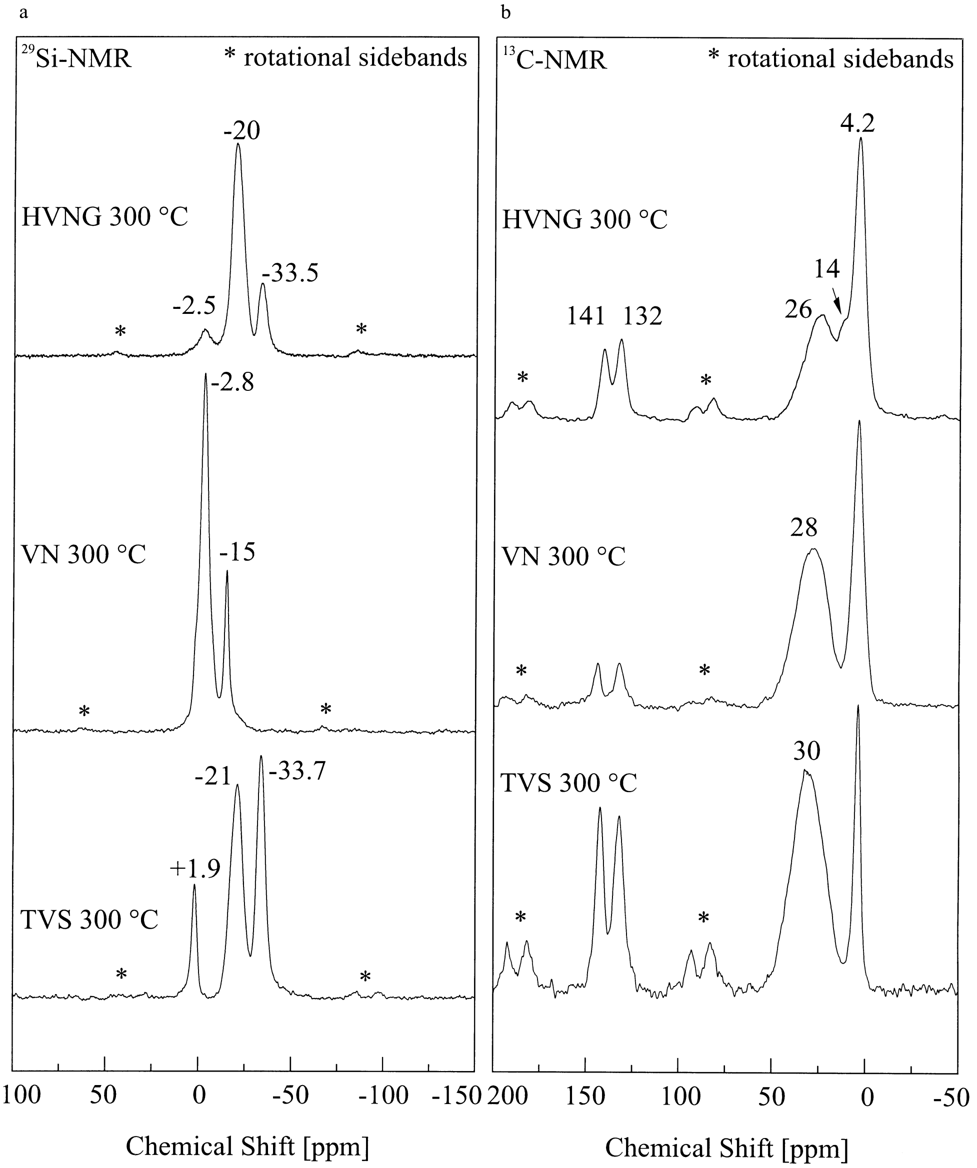

Fig. 4. (a) ^{29}Si- and (b) ^{13}C-NMR spectra of the crosslinked precursors HVNG (top), VN (middle) and TVS (bottom) annealed at 300°C.

gaseous species released in this temperature regime is methane, Fig. 2(b). This process is completed at 800°C and further structural changes are not detectable by FTIR spectroscopy anymore. In the FTIR spectrum recorded at this temperature only the absorption band corresponding to Si–H remains, indicating that there is still some amount of hydrogen present in the sample.

Changes in the structure of the solid intermediates during thermal treatment at temperatures beyond 300°C were also investigated by ^{29}Si and ^{13}C solid state NMR spectroscopy. Solid state NMR characterisation of a variety of silazanes has already been described,[12,18–20,22,23,25,27,32,35–38] but the assignment of the NMR resonances, especially of broad signals appearing in NMR spectra of crosslinked polymers and amorphous materials is difficult. In the present study we will use the peak assignment as reported in literature. Fig. 3(a) and (b) shows the NMR spectra of the precursor HVNG after different pyrolysis temperatures. The ^{29}Si spectrum of the crosslinked polymer cured at 300°C shows three sharp peaks. In addition to the signals at −20 and −33.5 ppm, assigned to silicon in $(\mathrm{N})_2\mathbf{Si}\mathrm{HMe}$ and $(\mathrm{N})_3\mathbf{Si}\mathrm{Vi}$ environments present in the liquid spectrum of the precursor, a new signal at —-2.5 ppm appears. Resonances having a ^{29}Si chemical shift in this range correspond to silicon atoms in $(\mathrm{N})_2\mathbf{Si}(\mathrm{C}^{\mathrm{sp}^3})_2$ sites and denoting crosslinking via hydrosilylation.[18,19,32] The ^{13}C spectrum at this temperature exhibits, in addition to the peaks arising from the carbons in the methyl- (4.2 ppm) and in the vinyl-group (132, 141 ppm), a broad signal at about 26 ppm and a shoulder at 14 ppm. Aliphatic carbon atoms causes ^{13}C resonances in this range indicating crosslinking via hydrosilylation and/or polymerisation of the vinyl groups.[18,20] An exact assignment of the signals appearing after crosslinking can be made only via comparison with the precursors TVS and VN.

Fig. 4(a) and (b) shows the ^{29}Si- and ^{13}C-NMR spectra of the precursors HVNG, VN and TVS after crosslinking at 300°C in comparison. The ^{13}C-NMR spectrum of precursor VN shows in addition to the sharp lines of the silylmethyl- (4.2 ppm) and the silylvinyl group (132/141 ppm) one broad line at about 28 ppm.[18,19,23] A peak at −2.8 ppm appears in addition to that at −15 ppm caused by $(N)_2\mathbf{Si}(CH_3)CH{=}CH_2$ sites in the ^{29}Si NMR spectrum.[18] In the ^{29}Si-NMR spectrum of the precursor TVS three signals are present. The peak at −33.7 ppm is caused by the initial $(N)_3\mathbf{Si}CH{=}CH_2$ environments.[18] The ^{29}Si resonance at −21 ppm is correlated to the crosslinking reaction. The third peak at 1.9 ppm, which is also present as a little shoulder in the ^{29}Si-NMR spectrum of the precursor VN, is assigned to $N\mathbf{Si}(Me)_3$ sites and is probably due to modifications of the polymer by the catalyst used.[22] The presence of a small amount of the end groups $(NSi(Me)_3)$ in the TVS precursor is also observed in the ^{13}C-NMR spectrum of this sample. In addition to the resonances caused by the carbons in the silylvinyl group, a sharp peak appears at 4.2 ppm corresponding to the carbons in these end groups.[19,23] The broad signal at about 30 ppm is again correlated to the crosslinking reaction. Since the crosslinking of TVS takes place exclusively via polymerisation of the vinyl groups, the resonance at 30 ppm (^{13}C) can be assigned to this reaction. The peak at −21 ppm in the ^{29}Si-NMR spectrum then corresponds to $(N)_3\mathbf{Si}C^{sp3}$ sites formed due to polymerisation. The signal at 28 ppm in the ^{13}C-NMR spectrum of the precursor VN also indicates that crosslinking takes place via polymerisation of the vinyl groups. For this reason, the ^{29}Si-NMR spectrum shows a peak at −2.8 ppm caused by $(N)_2\mathbf{Si}MeC^{sp3}$ sites. On the other hand, the ^{13}C-NMR spectrum of the crosslinked HVNG precursor shows two signals in addition to the resonances caused by the carbon atoms of the methyl- (4.2 ppm) and of the vinyl-groups (132/141 ppm). The broad peak at about 26 ppm must be in turn ascribed to the formation of aliphatic carbons due to crosslinking via polymerisation. The appearance of $(N)_2\mathbf{Si}MeC^{sp3}$ sites (−2.5 ppm) in the ^{29}Si-NMR spectrum also indicates that crosslinking takes place via hydrosilylation, though. Therefore, the shoulder observed at about 14 ppm in the ^{13}C-NMR spectrum of the HVNG polymer is caused by this reaction.

At 400°C (Fig. 3a and b), the peaks assigned to the vinyl group (^{29}Si: −33.5 ppm; ^{13}C: 132, 141 ppm) have disappeared in both the ^{29}Si- and the ^{13}C-spectrum of the HVNG-derived sample. This denotes that crosslinking via hydrosilylation and polymerisation as mentioned above is completed at this temperature. Further heating causes a broadening of all NMR lines. At 500°C, there is a slight high-field shift of the peaks (−2.5 ppm → −6 ppm; −20 ppm → −22 ppm) in the ^{29}Si spectrum in addition to a signal at −41 ppm appearing as a shoulder. The intensity of this shoulder increases with increasing temperature (600°C) and becomes the main peak (−45.5 ppm) at 700°C indicating environments close to $\mathbf{Si}N_3H$ and $\mathbf{Si}N_4$.[22,35] The high-field shift of the ^{29}Si peaks is corresponding to an increase of the number of Si−N bonds in contrast to the number of Si−C bonds, probably due to both the evolution of C-containing species (CH_4) and the segregation of carbon clusters. The chemical shift of the ^{13}C peak increases (4 ppm → 12 ppm) at 600°C. This is caused by the formation of $\mathbf{C}H_2Si_2$ sites.[32] Coincidentally, a new signal appears at 135 ppm which increases in intensity at 700°C. This indicates a high amount of sp^2-carbon in the form of carbon clusters, the so called free carbon.[20,23,25,27,32] In contrast, the ^{13}C spectrum of the precursor HVN with a factor of ten smaller concentration of vinyl groups heated at 700°C shows no signal at 135 ppm, Fig. 5. The vinyl groups of the precursor HVNG are therefore the reason for the occurrence of sp^2-carbon in the amorphous intermediate.

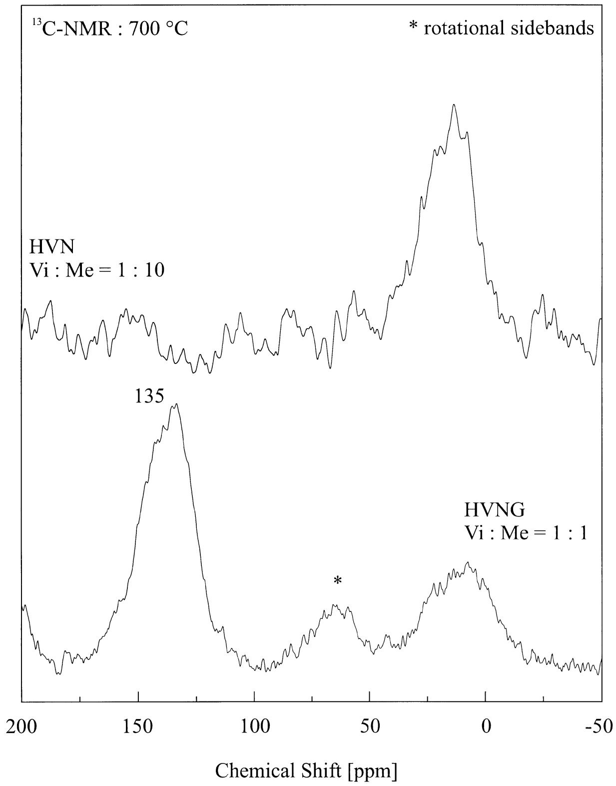

Fig. 5. ^{13}C-NMR spectra of (bottom) HVNG- and (top) HVN-derived amorphous Si–C–N–(H) ceramic annealed at 700°C. The comparison shows that there is no sp^2-carbon present in the amorphous material derived from HVN (vinyl concentration reduced by a factor of 10). In contrast to that there is a broad peak at about 135 ppm (according to sp^2-carbon) in the NMR spectrum of the HVNG-derived material.

3.3. Changes in the amorphous structure and crystallisation of the precursor HVNG (T = 1000–1700°C)

Pyrolysis at 1000°C finally yields an amorphous ceramic composed of a free carbon phase and a homogeneous Si–C–N–(H) phase, corresponding to one broad (width: 35 ppm) signal in the ^{29}Si spectrum, Fig. 6(a). The ^{13}C spectrum [Fig. 6(b)] is characterised by one peak (width: 40 ppm) at about 135 ppm corresponding to sp^2-carbon domains (free carbon).[20,23,25,27,32] The short spin lattice relaxation time indicates that paramagnetic centres (for example dangling bonds) are coupled to carbon in these domains. Further heating causes the formation of **C**Si$_4$ and **Si**N$_4$-environments with a short range order as can be seen in the appearance of a peak at 28 ppm in the ^{13}C spectrum and at −48 ppm in the ^{29}Si spectrum recorded on a sample heated at 1200°C.[32,35] At 1500°C, the ^{29}Si spectrum of the polymer derived ceramic shows three signals centred about −15, −30 and −48 ppm corresponding to **Si**C$_4$, **Si**N$_3$C and **Si**N$_4$ environments.[12,19,22,35–38] This indicates rearrangements in the amorphous state leading now to a heterogeneous Si–C–N phase. A density increase of 19.4% (2.3 g/cm^3 → 2.75 g/cm^3) and a mass loss of 4.7% in the temperature range between 800 and 1500°C accompanies this reorganisation. The continuous evolution of hydrogen containing species (which are still present, as shown by FTIR spectroscopy) is most probably responsible for this mass loss, therefore enabling the formation of SiN$_4$ and SiC$_4$ environments. Longer annealing times (48 h)

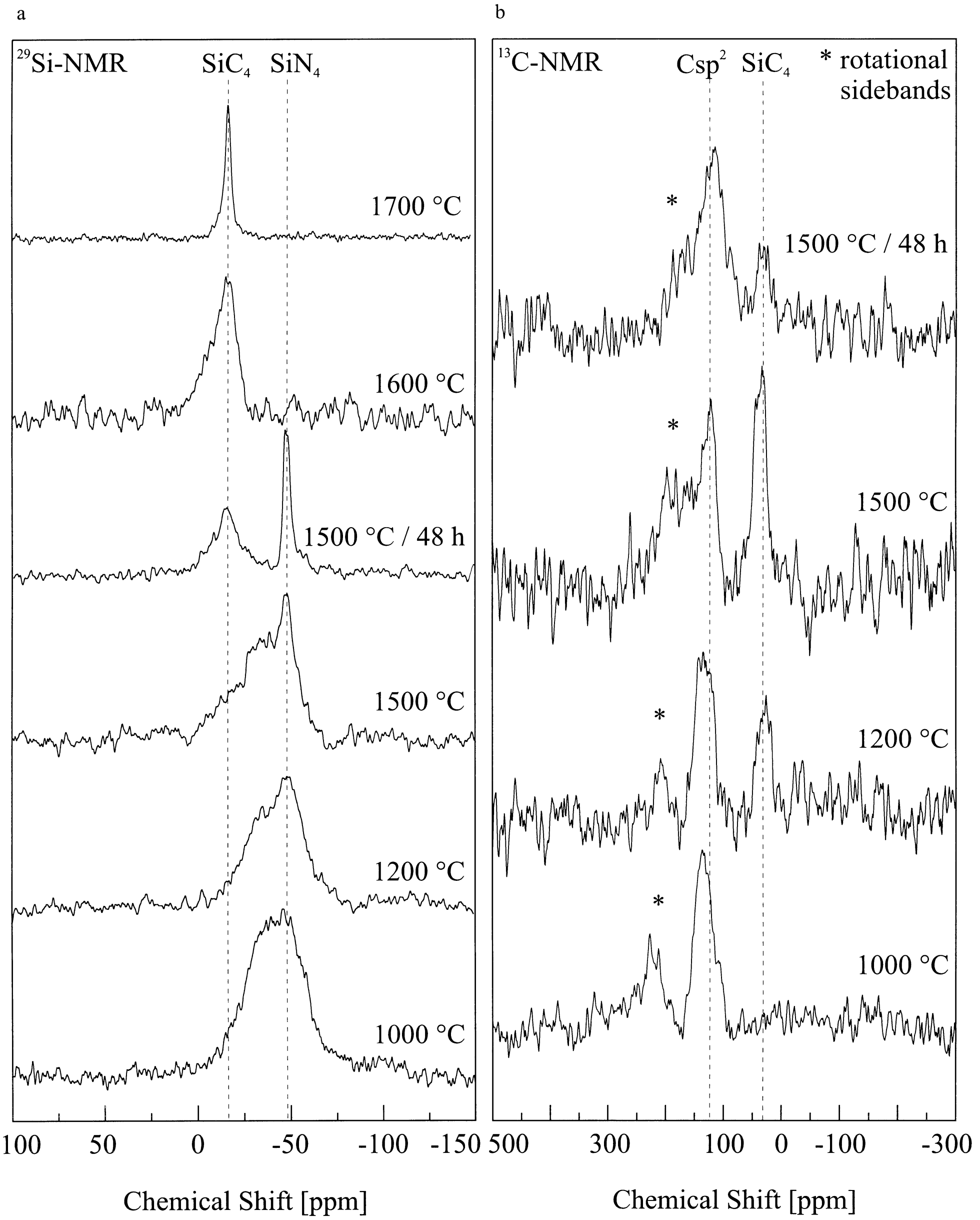

Fig. 6. (a) ^{29}Si- and (b) ^{13}C-NMR spectra of the pyrolytic residues of the precursor HVNG for increasing temperatures.

at 1500°C causes the formation of the thermodynamically stable crystalline phases SiC (−16 ppm) and Si_3N_4 (−48 ppm).[36,38] Crystalline SiC, especially β-SiC, is characterised by a long spin lattice relaxation time. This fact causes the decrease of the SiC peak in the ^{13}C spectra recorded on samples heated above 1500°C and evident the long range order of SiC, yet. At 1600°C, no Si_3N_4 but only a SiC signal is detected by ^{29}Si-NMR measurements, which becomes narrower at 1700°C indicating crystal growth of SiC. Upon crystallisation, density is increasing to 3.25 g/cm^3 (corresponding to SiC) with a substantial mass loss (26%) due to the decomposition of amorphous SiCN and Si_3N_4. These structural changes were particle size dependent, illuminating the importance of the kinetic aspects, Fig. 7. Using particles sizes >1 mm, the structural changes were shifted to higher temperatures, indicating that rearrangement is effected by both bond cleavage and diffusion of gaseous species. In contrast to the rearrangements and ordering phenomena detected in the NMR studies, XRD investigations (Fig. 8) showed amorphous patterns up to 1500°C. At 1500°C/48h broad diffraction peaks corresponding to nanocrystalline SiC and Si_3N_4 are observed in accordance with NMR results. At 1600°C only SiC is detectable. Si_3N_4 cannot be detected anymore at this temperature. At 1700°C the diffraction peaks become narrower indicating the increasing SiC crystallite size.

3.4. Comparison between HVNG, VN and TVS — polymer architecture and glass structure

In this section the effect of the precursor architecture on the structure of the amorphous ceramic preceding crystallisation is discussed. The precursors consist of tailored structural units, see Fig. 1. The polyvinylsilazane TVS consists of T-units only whereas the six-membered trimethyltrivinylcyclotrisilazane VN contains only D-units. In contrast, the precursor HVNG consists of mixed T- and D-units. The amorphous ceramic materials prepared by heating at 1500° were investigated by ^{29}Si-NMR spectroscopy; the spectra are shown in Fig. 9 in comparison.

The TVS derived ceramic shows one peak in the ^{29}Si spectrum at −48 ppm corresponding to SiN_4. This is most probably due to the fact that in the precursor Si is already bonded to three NH groups which upon pyrolysis may convert easily to a SiN_4 environment. On the other hand, there is a broad signal between 0 ppm and

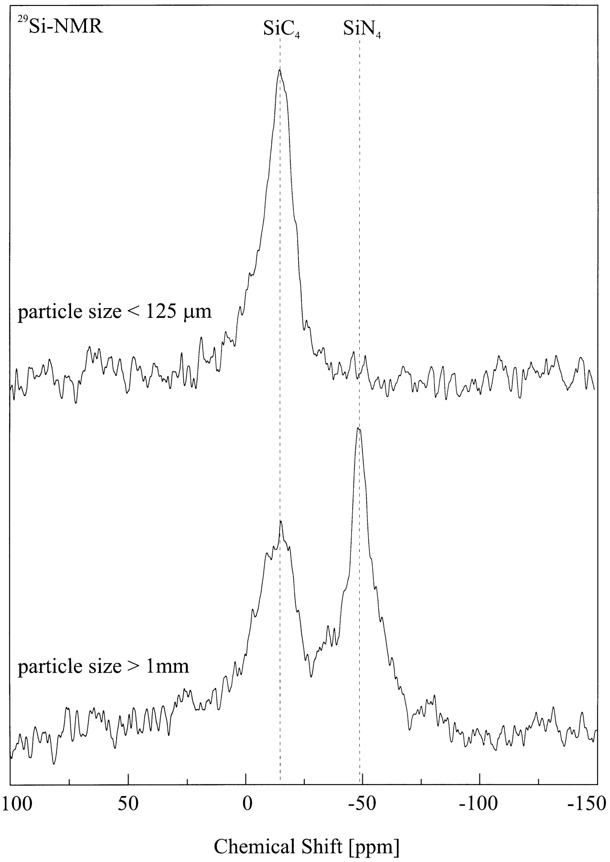

Fig. 7. ^{29}Si-NMR spectra of (bottom) a bulk sample (particle size >1 mm) and (top) of a powder sample (particle size <125 µm) heat treated at 1540°C.

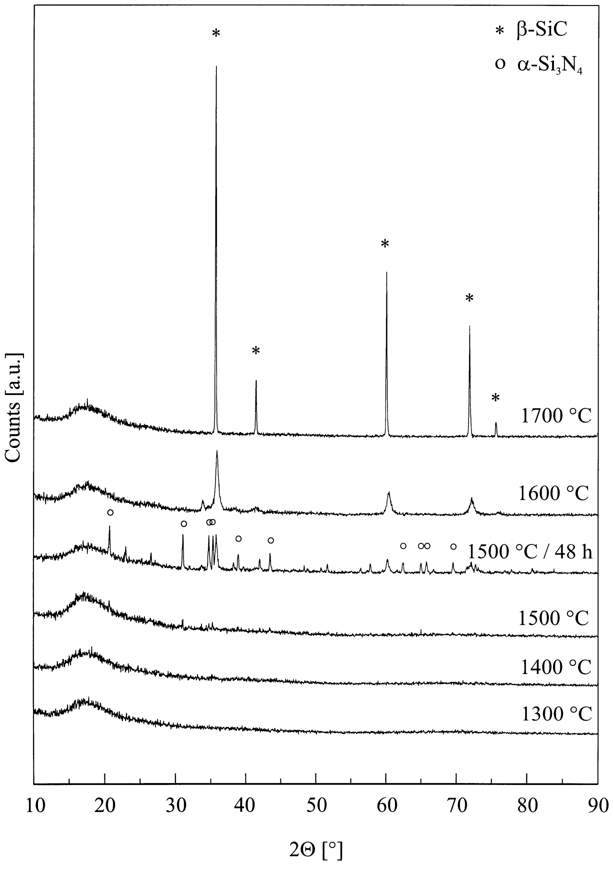

Fig. 8. X-ray powder diffraction patterns of the pyrolysed precursor HVNG annealed at different temperatures.

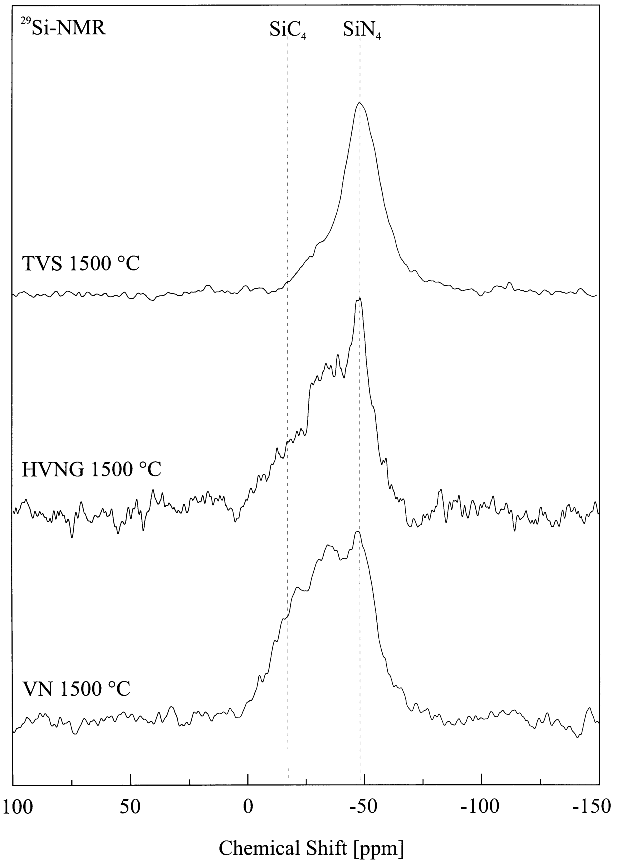

Fig. 9. ^{29}Si-NMR spectra of the amorphous Si–C–N ceramics derived from (top) TVS, (middle) HVNG and (bottom) VN by annealing at 1500°C. The comparison between the different amorphous materials shows that there is a correlation between the initial structural units of the precursors and the final microstructure of the amorphous ceramic.

65 ppm observed in the ^{29}Si-NMR spectrum of the amorphous material prepared from precursor VN. This indicates a broad distribution of $\mathbf{SiC}_x\mathrm{N}_{4-x}$ $(x = 0 - 4)$ sites. As described above, three distinguishable peaks at $-15/-30/-48$ ppm appear in the ^{29}Si spectrum of the HVNG derived material. This signals are assigned to SiC_4 (short range ordered), SiN_3C and SiN_4 (short range ordered) environments.

From these results we conclude that the presence of T-units is prestructuring the architecture of the TVS- and HVNG-polymers. Therefore, structural rearrangements during pyrolysis are limited, assuming that the Si–N(H) bonds are very stable. The six-membered VN-rings, however, consisting of D-units allow many possible changes in the structure during heating. This leads to a broader distribution of Si environments compared to the aforementioned precursors. The effect of these differences with respect to the crystallisation behaviour and the thermal stability of these polymer derived ceramics is still to be examined.

4. Conclusions

The pyrolysis of organometallic oligomers to amorphous ceramics and further crystallisation is understood only on a very basic level. Especially the correlation between precursor architecture and the structure of the amorphous material and its effect on the crystallisation behaviour is not known. In order to gain insight in the microstructural evolution, the structure of the solid residues derived from different tailored preceramic oligomers has to be characterised and compared with each other.

We characterised the precursor HVNG consisting of mixed D- and T-units particularly via solid state ^{29}Si- and ^{13}C-NMR spectroscopy and compared the results with those obtained from the amorphous intermediates derived from TVS (containing T-units) and VN (containing D-units).

The transformation of the HVNG precursor prepared from di- and trifunctional chlorosilanes to an amorphous and finally a crystalline ceramic can be described as follows:

1. thermal crosslinking via polymerisation of the vinyl groups and hydrosilylation reaction, completed at 400°C;
2. organic/inorganic transition between 500 and 800°C yielding a free carbon phase (due to the presence of vinyl groups in the precursor) and a homogeneous amorphous Si−C−N−(H) phase;
3. structural rearrangements between 800 and 1500°C, possibly effected by the elimination of hydrogen containing species, leading to the formation of sp^2-carbon domains and to a phase separation (SiC_4, $SiCN_3$, SiN_4) in the amorphous state;
4. decomposition of the amorphous ceramic, above 1500°C, yielding mainly crystalline SiC as the only phase.

The comparison between HVNG, VN and TVS showed significant differences in the NMR spectra of the amorphous materials at 1500°C indicating a correlation of the polymer architecture with the structure of the amorphous ceramic. This becomes evident especially from ^{29}Si spectra. Precursor TVS (T-units) yields an amorphous pyrolysis residue containing mainly SiN_4 sites whereas the pyrolysis of the polymer VN consisting of D-units leads to an amorphous ceramic which contains a broad distribution of SiC_xN_y environments. Hence, the presence of trifunctional units (T-units) limits structural rearrangements and restricts the posssible Si environments whereas difunctional units (D-units) enable a broader distribution of Si sites. If these results are confirmed at the examination of similar systems, this has far-reaching consequences at the estimate of the thermal stability of amorphous Si–C–N ceramics.

Acknowledgements

The authors wish to thank W. Weibelzahl for the coupled TG/FTIR and bulk density measurements.

References

1. Messier, D. R. and Croft, W. J., In *Preparation and Properties of Solid-State Materials*, Vol. 7, ed. W. R. Wilcox. Marcel Dekker, New York, 1982.
2. Ziegler, G., Heinrich, J. and Wötting, G., Review: relationship between processing, microstructure and properties of dense and reaction-bonded silicon nitride. *J. Mater. Sci.*, 1987, **22**, 3041–3086.
3. Verbeek, W. and Winter, G., Offenlegungsschrift 2236078, 1974.
4. Yajima, S., Okamura, K., Hayashi, J. and Omori, M., Synthesis of continuous SiC fibres with high tensile strength. *J. Am. Ceram. Soc.*, 1976, **59**, 324–327.
5. Rice, R. W., Ceramics from polymer pyrolysis, opportunities and needs — a materials perspective. *Am. Ceram. Soc. Bull.*, 1983, **62**, 889–892.
6. Seyferth, D., Strohmann, C., Tracy, H. J. and Robison, J. L., Synthesis and useful reactions of organosilicon polymeric precursors for ceramics. *Mat. Res. Soc. Symp. Proc.*, 1992, **249**, 3–14.
7. Riedel, R. and Dressler, W., Chemical Formation of Ceramics. *Ceram. Inter.*, 1996, **22**, 233–239.
8. Ziegler, G., Hapke, J. and Lücke, J., Processing of CMC's from novel organometallic precursors. *Ceram. Trans.*, 1995, **58**, 13–23.
9. Keuthen, M., Lücke, J., Schönfelder, H. and Ziegler, G., Oxidationsbeständige Hochtemperaturbauteile auf der Basis von faserverstärktem SiC über Infiltration und Pyrolyse flüssiger Keramikprecursoren. In *Proc. Symp. Neue Werkstoffe in Bayern*, Erlangen, 1994.
10. Mucalo, M. R., Milestone, N. B., Vickridge, I. C. and Swain, M. V., Preparation of ceramic coatings from preceramic precursors. *J. Mat. Sci.*, 1994, **29**, 4487–4499.
11. Pouskouleli, G., Metallorganic compounds as preceramic materials I. Non-Oxide Ceramics. *Ceram. Int.*, 1989, **15**, 213–229.
12. Peuckert, M., Vaahs, T. and Brück, M., Ceramics from organometallic polymers. *Adv. Mater.*, 1990, **2**, 398–404.
13. Schilling, C. L. Jr., Wesson, J. P. and Williams, T. C., Polycarbosilane precursors for silicon carbide. *Am. Ceram. Soc. Bull.*, 1983, **62**, 912–915.
14. Hapke, J. and Ziegler, G., Synthesis and properties of liquid organometallic precursors for advanced Si–Ti–C–N Composites. *Adv. Mater.*, 1995, **7**, 380–384.
15. Birot, M., Pillot, J.-P. and Dunogues, J., Comprehensive chemistry of polycarbosilanes, polysilazanes and polycarbosilazanes as precursors of ceramics. *Chem. Rev.*, 1995, **95**, 1443–1477.
16. Funayama, O., Kato, T., Tashiro, Y. and Isoda, T., Synthesis of a polyborosilazanes and its conversion into inorganic compounds. *J. Am. Ceram. Soc.*, 1993, **76**, 717–723.
17. Lücke, J., Hacker, J., Suttor, D. and Ziegler, G., Synthesis and characterization of silazane-based polymers as precursors of ceramic matrix composites. *Appl. Organomet. Chem.*, 1997, **11**, 184–194.
18. Choong Kwet Yive, N. S., Corriu, R., Leclercq, D., Mutin, P. H. and Vioux, A., Polyvinylsilazane: a novel precursor to silicon carbonitride. *New J. Chem.*, 1991, **15**, 85–92.
19. Mocaer, D., Paille, R., Naslain, R., Richard, C., Pillot, J.-P., Dunogues, J., Gerardin, C. and Taulelle, F., Si–C–N Ceramics with high microstructural stability elaborated from the pyrolysis of new polycarbosilazanes precursors, Part I. The organic/inorganic transition. *J. Mat. Sci.*, 1993, **28**, 2615–2631.
20. Gerardin, C., Taulelle, F. and Livage, J., Pyrolysis of a polyvinylsilazane, polymeric precursor for silicon carbonitride: structural investigation by ^{1}H, ^{13}C, ^{29}Si, ^{15}N and ^{14}N nuclear magnetic resonance. *J. Chim. Phys.*, 1992, **89**, 461–467.
21. Seyferth, D. and Wiseman, G. H., High-yield synthesis of Si_3N_4/SiC ceramic materials by pyrolysis of a novel polyorganosilazane. *J. Am. Ceram. Soc.*, 1984, **14**, C132–133.
22. Lewis, R. H. and Maciel, G. E., Magnetic resonance characterization of solid-state intermediates in the generation of ceramics by pyrolysis of hydridopolysilazane. *J. Mat. Sci.*, 1995, **30**, 5020–5030.
23. Brodie, N., Majoral, J.-P. and Disson, J.-P., An NMR study of the step by step pyrolysis of a polysilazane precursor of silicon nitride. *Inorg. Chem.*, 1993, **32**, 4646–4649.
24. Zhang, Z.-F., Babonneau, F., Laine, R. M., Mu, Y., Harrod, J. F. and Rahn, J. A., Poly(methylsilane) — a high ceramic yield precursor to silicon carbide. *J. Am. Ceram. Soc.*, 1991, **74**, 670–673.
25. Soraru, G. D., Babonneau, F. and Mackenzie, J. D., Structural evolutions from polycarbosilane to SiC ceramic. *J. Mat. Sci.*, 1990, **23**, 3886– 3893.
26. Bahloul, D., Pereira, M., Goursat, P., Choong Kwet Yive, N. S. and Corriu, R. J. P., Preparation of silicon carbonitrides from an organosilicon polymer: I, thermal decomposition of the cross-linked polysilazane. *J. Am. Ceram. Soc.*, 1993, **76**, 1156–1162.
27. Laine, R. M., Babonneau, F., Blowhowiak, K. Y., Kennish, R. A., Rahn, J. A., Exarhos, G. J. and Waldner, K., The evolutionary process during pyrolytic transformation of poly(*N*-methylsilazane) from a preceramic polymer into an amorphous silicon nitride/carbon composite. *J. Am. Ceram. Soc.*, 1995, **78**, 137–145.
28. Lavedrine, A., Bahloul, D., Goursat, P., Choong Kwet Yive, N. S., Corriu, R., Leclercq, D., Mutin, H. and Vioux, H., Pyrolysis of polyvinylsilazane precursors to silicon carbonitride. *J. Euro. Ceram. Soc.*, 1991, **8**, 221–227.
29. Roux, P., Pillot, J.-P., Birot, M., Dunogues, J. and Richard, C. Structural effects in the thermal crosslinking of modell polycarbosilazanes. 6th Europ. Conf. Compos. Mat., Bordeaux (1992).
30. Monthioux, M. and Delverdier, D., Thermal behavior of (organosilicon) polymer-derived ceramics. V: main facts and trends. *J. Euro. Ceram. Soc.*, 1996, **16**, 721–737.
31. Laine, R. M., Babonneau, F., Rahn, J. A., Zhang, Z.-F. and Youngdahl, K. A. The effect of monomer architecture on selectivity to ceramic products and microstructure in silicon preceramic polymers. 37th Sagamore Army Mater. Res. Conf. Proc. ed. D. J. Viechnicki. Publicity Department of the US Army, 1991.
32. Seitz, J., Bill, J., Egger, N. F. and Aldinger, A., Structural investigations of Si/C/N-ceramics from polysilazane precursors by nuclear magnetic resonance. *J. Euro. Ceram. Soc.*, 1996, **16**, 885–891.
33. Bendall, M. R. and Gordon, R. E., Depth and refocusing pulses designed multipulse NMR with surface coils. *J. Magn. Res.*, 1983, **53**, 365–385.
34. Weidlein, J., Müller, U. and Dehnicke, K., Schwingungsfrequenzen, 1. Aufl., Band 1 (Hauptgruppenelemente), Georg Thieme Verlag, Stuttgart, New York, 1981.

35. Hatfield, G. R. and Carduner, K. R., Review: solid state NMR: applications in high performance ceramics. *J. Mat. Sci.*, 1989, **24**, 4209–4219.
36. He, J., Scarlete, M. and Harrod, J. F., Silicon nitride and silicon carbonitride by the pyrolysis of poly (methylsiladiazane). *J. Am. Ceram. Soc.*, 1995, **78**, 3009–3017.
37. Apperley, D. C., Harris, R. K., Marshall, G. L. and Thompson, D. P., Nuclear magnetic resonance studies of silicon carbide polytypes. *J. Am. Ceram. Soc.*, 1991, **74**, 777–782.
38. Carduner, K. R., Blackwell, C. S., Hammond, W. B., Reidinger, F. and Hatfield, G. R., ^{29}Si NMR characterization of α- and β-silicon nitride. *J. Am. Ceram. Soc.*, 1990, **112**, 4676–4679.